AIAA JOURNAL
Vol. 33, No. 10, October 1995

Nonequilibrium-Dissociated Stagnation Boundary-Layer Flow on an Arbitrarily Catalytic Swept Wing

George R. Inger*
Iowa State University, Ames, Iowa 50011

The aerodynamic heating of a swept stagnation line is examined in the high-altitude hypersonic flight regime where nonequilibrium dissociation/recombination in the boundary layer and finite surface catalysis effects are both important. Assuming a highly cooled body ($T_w/T_s \ll 1$), we extend Fay and Riddell's well-known self-similar solution for nonequilibrium-dissociated flow to include the effects of sweepback and arbitrary surface catalycity. Specific results for heat transfer are presented for the same zero sweep baseline case that was used in Fay and Riddell's work. In the frozen gas-phase limit, it is found that the combined net effects of sweep angle Λ wipe out the dissociation effects altogether beyond about $\Lambda \approx 65$ deg and thus eliminate the usual favorable effect of a noncatalytic wall in reducing nonequilibrium heat transfer. Regarding the gas-phase chemistry aspect, results for a completely noncatalytic wall show that notwithstanding the significant spanwise viscous dissipation heating effect on the dissociation rate the net sweep effect diminishes the gas-phase reaction effect to zero beyond $\Lambda \approx 60$ deg, analogously to the surface reaction case.

Nomenclature

C_D = equilibrium constant, Eq. (8a)
$\hat{C}_p$ = specific heat of molecules
f = boundary-layer velocity similarity function, Eq. (2)
G = composition-dependent portion of reaction rate, Eq. (8)
h_D = specific dissociation energy of molecules
K_w = speed of catalytic atom recombination on body surface
k_r' = recombination rate constant
Le = Lewis number, Pr/Sc
Pr = Prandtl number
p = static pressure
Q_w = nondimensional heat transfer rate, Eq. (10)
q_w = surface heat transfer rate per unit area
R_m = molecular gas constant
R_u = universal gas constant
$\mathcal{R}$ = net reaction rate distribution function, $\theta^{\omega-2}G$, Eq. (8)
Sc = Schmidt number
s = w/w_e
T = absolute temperature
U_∞ = freestream (flight) velocity
u, w = chordwise, spanwise velocity components
x, y, z = coordinates in streamwise, normal, and spanwise directions
α = atom mass fraction
β_s = inviscid flow stagnation point velocity gradient, $(du_e/dx)_s$
Γ_c = Dähmkohler number for surface reactions
$\bar{\Gamma}_c$ = $\Gamma_c/0.47\mathrm{Sc}^{1/3}$
Γ_G = Dähmkohler number for gas-phase recombination
γ = specific heat ratio
γ_c = catalytic efficiency of wall material
η = boundary-layer similarity coordinate
θ = T/T_e
θ_D = nondimensional dissociation temperature, $h_D/(R_m T_e)$
Λ = sweepback angle
μ = coefficient of viscosity
ρ = mixture density
τ_0 = $R_m\theta_{D_0}/\hat{C}_{p_0}$
ω = recombination rate temperature-dependence exponent, as in $k_r = k_r' T^\omega$

Subscripts

e = boundary-layer edge conditions
eq = value for equilibrium boundary-layer flow
F = value for frozen boundary-layer flow
M = molecule
s = inviscid flow conditions at stagnation point
w = conditions on body surface
0 = conditions at zero sweep
∞ = freestream conditions
$()'$ = $\partial()/\partial\eta$

Presented as Paper 94-2072 at the AIAA/ASME 6th Joint Thermophysics and Heat Transfer Conference, Colorado Springs, CO, June 20–23, 1994; received July 20, 1994; revision received March 27, 1995; accepted for publication April 6, 1995.

*Professor, Department of Aerospace Engineering and Engineering Mechanics. Associate Fellow AIAA.

Introduction

THE interest in aerodynamically efficient hypersonic vehicle configurations has led to recently proposed new applications to lifting atmospheric flight, orbital transfer, and planetary atmosphere entry. In such applications, the question of high-aerodynamic heating in certain areas of the configuration is an important aspect of the design analysis, as are high-temperature dissociation effects on this heating. Moreover, owing to the combination of high-flight speeds (short flow residence times) and lower density high-altitude operating conditions (long chemical reaction collision times), such dissociation effects can involve marked departures from gas-phase chemical equilibrium in the boundary layer and finite rates of catalytic atom recombination along the vehicle surface. These nonequilibrium effects in turn cause significant reductions in aerodynamic heating if the body surface is not fully catalytic.[1] Consequently, it is appropriate to address the issue of predicting the nonequilibrium heat transfer rates to key regions on the vehicle and how these depend on the catalytic properties of the surface material.

The present paper deals with this issue for the special but important problem of the stagnation line along a swept wing (Fig. 1). The body is taken to be highly cooled ($T_w/T_s \ll 1$) and the boundary layer along it to be laminar and steady. Our goal is to give a solution for the combined gas-phase/surface catalytic nonequilibrium effects on the heat transfer which extends the well-known self-similar solution of Fay and Riddell[1] to include the effects of sweepback and arbitrary surface catalycity. Such an extension is particularly worthwhile since their work has become a standard of reference in the aerodynamic heating literature. We also give a closed-form solution for arbitrarily catalytic surfaces in the frozen gas-phase limit that extends Goulard's earlier work[2] to swept-back flow conditions. The present approach has a significant analytical flavor rather than being

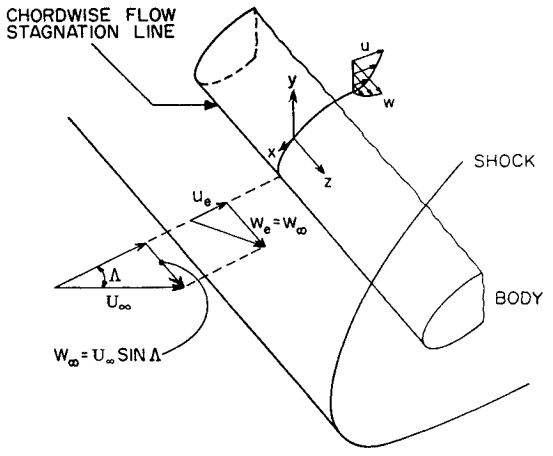

Fig. 1 Swept wing leading edge region: a reattachment line with sweep-induced crossflow.

purely numerical, in order to provide results that can serve advanced engineering design analysis, illuminate the relative role of kinetic rates and surface catalysis, and provide a basis for computational fluid dynamics (CFD) code result validation.

Formulation of the Analysis

We consider airflow in the shock layer around a highly cooled body under such hypervelocity flight conditions that the postshock dissociative and vibrational chemistry can be taken as fully equilibrated upon reaching the boundary-layer edge. That is, we confine attention to that range of altitude/speed flight conditions where there is a distinct inviscid shock layer region across which the dissociative relaxation time is very short compared to the reaction time within either the underlying boundary layer or upon the body surface. This boundary-layer regime, which pertains to flight altitudes below 200–250 K-ft (depending on body size), still contains a large amount of the interesting nonequilibrium dissociation effects on heating before the onset of dissociative nonequilibrium in the fully viscous shock layer regime (see Chung[3] on this point, especially Fig. 6 therein).

The analysis may be further expedited without loss of the essential nonequilibrium flow thermophysics by introducing the following simplifying assumptions.[4] 1) As far as heat transfer is concerned, the gas mixture can be adequately approximated by a binary mixture of atoms and molecules with equal specific heats and negligible thermal diffusion between them. 2) The Prandtl and Lewis numbers are near unity and, like the viscosity-density product, are constant across the boundary layer. 3) The chemical reaction effects on the boundary-layer velocity profile solutions (via the reciprocal density coefficient of the pressure gradient term in the momentum equations) are small enough for a highly cooled wall to permit taking these profiles as known distributions in the leading approximation. 4) Catalytic recombination of atoms on the body surface is governed by a first-order rate law with negligible heterogeneous dissociation.[2] 5) The freestream is strongly hypersonic, since the dissociation effects of interest here only occur at such flight speeds.

We consider the immediate vicinity of the stagnation line on the leading edge of an infinite span swept wing (Fig. 1), where the flow is self-similar with a nonzero spanwise inviscid velocity $w_e = U_\infty \sin \Lambda$. For such a flow it is convenient to introduce the similarity coordinate[5]

$$\eta = \sqrt{\frac{\beta_s}{\rho_w \mu_w}} \int_0^y \rho \, dy \tag{1}$$

plus the following nondimensional chordwise (x) and spanwise (z) velocity and temperature variables:

$$u/u_e = \frac{\partial f}{\partial \eta} \cong f'(\eta) \tag{2}$$

$$w/w_e = s(\eta) \tag{3}$$

$$T/T_e = \theta(\eta) \tag{4}$$

where $u_e = \beta_s x$ and $T_e = T_s$ in the stagnation region. Then under the aforementioned flow model simplifications, $s \cong f'$ (Ref. 6) with f' regarded as a known boundary-layer profile function, and the thermochemistry is governed by the pair of equations

$$S_c f \alpha' + \alpha'' = \mathcal{R}(\alpha, \theta) \tag{5}$$

$$\theta \cong \theta_w + (1 - \theta_w) \cdot Pr^{\frac{1}{3}} f' + (\sqrt{Pr}/2C_p T_e) \times \left[u_e^2 \left(f' \cdot Pr^{\frac{1}{3}} - f'^2 \right) + w_e^2 \left(f' \cdot Pr^{\frac{1}{3}} - s^2 \right) \right] + (h_D / \hat{C}_p T_e) \left[(\alpha_e - \alpha_w) f' \cdot Sc^{\frac{1}{3}} + \alpha_w - \alpha \right] \tag{6}$$

where the latter equation is obtained from the generalized Crocco energy equation integral pertaining to highly cooled wall conditions.[7]

The term $\mathcal{R}(\alpha, \theta)$ on the right side of atomic specie conservation Eq. (5) is the nondimensional net gas-phase recombination rate; for a binary mixture of atoms and molecules undergoing the dissociation-recombination reaction

$$A_2 + X \underset{k_r}{\overset{k_d}{\rightleftarrows}} 2A + X \tag{7}$$

(where A_2, A, and X denote a molecule, atom, and any third body, respectively, and $k_r = k_r' T^\omega$ is the recombination rate) this function is

$$\mathcal{R} = \Gamma_G \cdot \theta^{\omega - 2} \left[\frac{\alpha^2}{1 + \alpha} - \frac{C_D}{p_e} (1 - \alpha) e^{-\theta_D/\theta} \right] \equiv \Gamma_G \cdot G(\alpha, \theta) \tag{8a}$$

Here C_D is an equilibrium constant and Γ_G is a characteristic local flow time/gas-phase reaction time ratio (Dähmkohler number) defined by

$$\Gamma_G \equiv \frac{2 k_r' Sc T_s^{\omega - 2} p_s^2}{\beta_s R_u^2} \tag{8b}$$

The function $\theta^{\omega-2}$ in Eq. (8a) represents the temperature profile effect on the recombination rate and pre-exponential portion of the dissociation rate; since $\omega \cong -1.5$ for air, this effect has a considerable influence on the nonequilibrium behavior across a highly cooled boundary layer.[4] The function $G(\alpha, \theta)$ represents the composition-dependence of the reaction rate and involves a contribution from both the local recombination ($\sim \alpha^2$) and dissociation rates; it vanishes identically when the boundary layer is in equilibrium ($\Gamma_G \to \infty$) but does not in the opposite extreme of chemically frozen flow ($\Gamma_G \to 0$).

The boundary conditions at the edge of the boundary layer ($\eta \to \infty$) are that $f'(\infty) = \theta(\infty) = 1$ along with the inviscid equilibrium-dissociation condition $G(\xi, \infty) = 0, \alpha = \alpha_e = \alpha_{eq}(T_e)$ where $\alpha_e^2 = (1 - \alpha_e^2) C_D e^{-\theta_D} / p_e$. Along the arbitrarily catalytic cold impermeable wall surface, $\theta(\xi, 0) = \theta_w \ll 1$ and $s(\xi, 0) = f(\xi, 0) = f'(\xi, 0) = 0$ for no velocity or thermal slip. Furthermore, there is the atomic specie boundary condition

$$\alpha'(0) = \sqrt{\frac{\rho_w \mu_w}{\beta s}} \frac{Sc K_w}{\mu_w} \cdot \alpha(0) \equiv \Gamma_c \cdot \alpha_w \tag{9}$$

where Γ_c is the characteristic local diffusion time to recombination time ratio (or heterogeneous Dähmkohler number) expressed in terms of the atom recombination velocity K_w on the surface. The parameter K_w is a known function of the wall temperature and material that is related to the surface catalytic efficiency γ_c by $\gamma_c \equiv (\pi K_w^2 / R_m T_w)^{1/2}$. The boundary condition (9) expresses the fact that the rate of diffusion of atoms from the gas is balanced by the rate of catalytic recombination on the wall surface. When $\Gamma_c \to \infty$ the surface is completely catalytic [$\alpha(0) = 0$], whereas in the other extreme $\Gamma_c = 0$ the surface is noncatalytic and the wall atom diffusion vanishes [$\alpha'(0) = 0$].

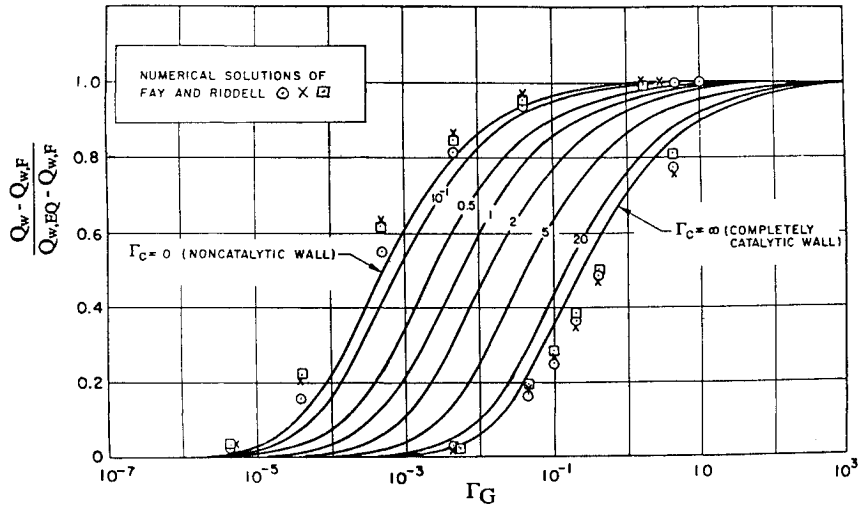

Fig. 2 Comparison of present solution for unswept nonequilibrium stagnation heat transfer vs numerical results of Fay and Riddell[1]; $\theta_{w_0} = 0.04$, $Sc = 0.5$, $Pr = 0.7$, $\omega = -1.5$, $\theta_{D_0} = 5$, $\alpha_{s_0} = 0.536$.

Once the foregoing split boundary value problem for $\alpha(\eta)$ is solved, the corresponding nondimensional wall heat transfer rate may be determined from

$$Q_w \equiv \frac{-Pr(\dot{q}_w/\hat{C}_p T_e)}{\sqrt{\rho_w \mu_w u_e[(d\xi/dx)/2\xi][1+r]}} = \theta'(0) + \frac{L_e h_D}{\hat{C}_p T_e} \cdot \alpha'(0) \tag{10}$$

Clearly, only heat conduction contributes to the heat transfer when the wall is completely noncatalytic [$\alpha'(0) = 0$].

The foregoing formulation represents a generalization of the Fay and Riddell's well-known nonequilibrium stagnation boundary-layer theory[1] to embrace arbitrary surface catalycity and the effects of sweepback. It encompasses the entire extent of nonequilibrium/finite wall catalycity effects depending on the individual values of the two Dähmkohler number parameters Γ_G and Γ_c, respectively. For example, the limit $\Gamma_G \gg 1$ corresponds to equilibrium-dissociation behavior throughout the boundary layer giving $\dot{q}_w = \dot{q}_{w,eq}$. The opposite limit $\Gamma_G \to 0$ pertains to a chemically frozen (nonreacting) boundary layer with a heat transfer rate from Eq. (10) that is highly dependent on the degree of finite wall catalycity reflected in the value of Γ_c.

Solution Method and Validation

The differential Eq. (5) for atomic specific conservation plus the accompanying energy Eq. (6) were solved by a standard finite difference method (e.g., see Ref. 8). In this method, the equations are linearized about an initial guess, put in finite difference form, and the resulting tridiagonal matrix problem solved for the values of α and θ at each of the η-mesh points within the boundary layer. The solutions so obtained are then used as new initial profiles in the next iteration where the matrix is solved again, this sequence being repeated until convergence to a final solution to the original nonlinear equations is obtained. Care was taken to establish both convergency and accuracy: with a $\Delta\eta = 0.1$ mesh size in the range $0 \le \eta \le 5$, it was found that 50 iterations were generally sufficient to establish an initial profile-independent converged answer with an error in α and each of the equation terms of less than 10^{-5}. Solutions were carried out satisfactorily over many values of the various thermochemical parameters and both gas-phase and surface catalysis Dähmkohler numbers, from sweep angles ranging from zero to 80 deg.

The author could find no previous systematic numerical results nor pertinent experimental data for swept wing nonequilibrium-dissociated viscous flow with which the present study could be compared. Our results can be validated in the zero sweep case, however, as shown in Fig. 2, where good agreement is indicated with Fay and Riddell's predictions of both wall atom concentration and heat transfer throughout the entire nonequilibrium regime for either a fully catalytic or completely catalytic wall. A further supporting comparison is illustrated in Fig. 3, where the nonequilibrium heat transfer vs altitude is shown for a typical case as a function of various assumed values of the wall catalytic efficiency: the resulting significant reduction in heating predicted by the present theory for moderately to weakly catalytic walls is seen to be in good agreement with Chung's exact numerical solutions based on fully viscous shock layer theory.[3]

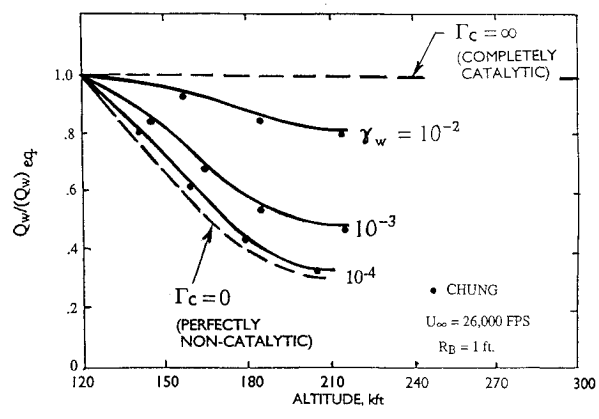

Fig. 3 Predicted unswept nonequilibrium heat transfer variation with altitude for various surface catalytic efficiencies: comparison with Chung's viscous shock layer solutions.[3]

Sweepback Effect on Nonequilibrium Boundary-Layer Properties

To understand the swept solution results, it is important to note that the aerothermochemical aspects of the problem can be influenced by sweepback in three ways. First, sweep significantly alters the equilibrium-dissociated inviscid flow at the edge of the boundary layer. As shown by the thermodynamic and energy relations which govern this (see the Appendix), sweep rapidly reduces both the dissociation level $\alpha_e = \alpha_s$ and (especially) the static temperature T_s on the stagnation line, along with the usual $\cos^2 \Lambda$ reduction in static pressure, see Fig. 4. Such reductions tend to suppress both the recombination and dissociation rates in the gas phase. Second, sweepback alters the magnitudes of the basic Dähmkohler numbers Γ_G and Γ_c that control the relative degree of nonequilibrium in the gas-phase and surface catalysis reactions, respectively. This is due to the combined effects on the inviscid gas state and on the chordwise stagnation velocity gradient which is proportional to $\cos \Lambda$ (Ref. 9). Considering the gas-phase reaction parameter, we find for $\omega = -1.5$ that

$$\frac{\Gamma_G}{(\Gamma_G)_{\Lambda=0}} \cong \frac{T_s^\omega/\beta_s}{\left[T_s^\omega/\beta_s\right]_{\Lambda=0}} \cong (\cos\Lambda)^{2\omega-1} \cong \sec^4 \Lambda \tag{11}$$

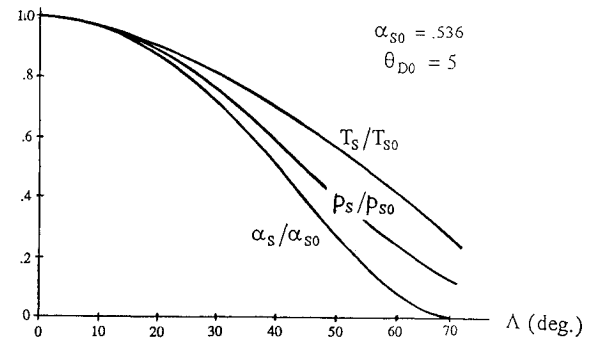

Fig. 4 Typical sweepback effects on inviscid equilibrium properties.

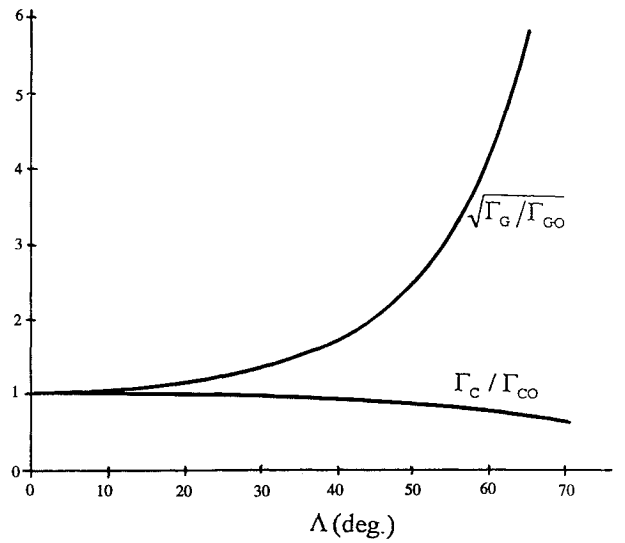

Fig. 5 Sweepback effects on the gas-phase and surface catalysis Dähmkohler numbers.

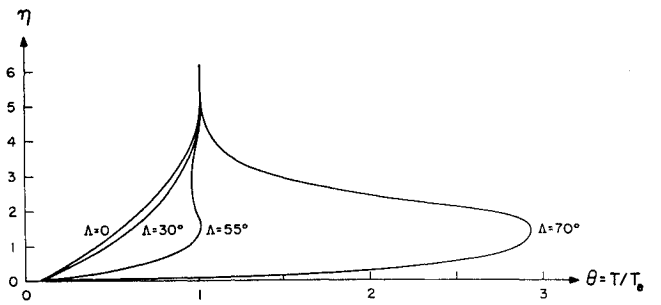

Fig. 6 Sweepback effects on boundary-layer temperature profiles.

since $p_s/p_{s_0} = \cos^2 \Lambda$, and $T_s/T_{s_0} \leq \cos^2 \Lambda$. At $\Lambda = 60$ deg, for example, this predicts an order of magnitude increase (Fig. 5), indicating that large crossflow drives the gas-phase reactions in the boundary layer toward equilibrium when recombination is dominant. Turning to the surface recombination parameter Γ_c, a similar type of analysis for a fixed wall temperature shows that

$$\Gamma_c/(\Gamma_c)_{\Lambda=0} = \cos^{\frac{1}{2}} \Lambda \tag{12}$$

implying that sweep slightly reduces the effective catalycity of the wall (Fig. 5). Third, the viscous dissipation heating associated with the spanwise boundary layer [i.e., the term $\sim w_e^2$ in Eq. (6)] can significantly affect the gas-phase reaction within the boundary layer, especially the dissociation rate. Consider Fig. 6, where typical boundary-layer temperature profiles are illustrated for various sweep angles. When the sweep angle is small to moderate and the crossflow dissipation heating is thus small, the temperature drops monotomically inward across the boundary layer, and the nonequilibrium gas-phase reaction is dominated by recombination ($\sim\theta^{\omega-2}\alpha^2$) near the cold surface. On the other hand, at large sweep angles $\Lambda > 60$ deg the crossflow dissipation causes a pronounced temperature overshoot, and this can significantly affect the dissociation rate in the vicinity of this temperature maximum because of its exponential dependence ($\sim e^{-\theta_D/\theta}$).

Guided by the foregoing remarks, we now present typical results for the predicted sweepback effect on the nonequilibrium boundary-layer properties of wall atom concentration and heat transfer. To make the point, we have chosen for study the same zero sweep baseline case that was employed in Fay and Riddell's work: $\alpha_{s0} = 0.536$, $\theta_{D_0} = 5.0$, $\theta_{w0} = 0.04$.

Frozen Boundary-Layer Flow

The first set of results deals with the influence of finite surface catalysis only, for the limiting case of chemically frozen gas phase reaction ($\Gamma_G = 0$). Here, Eq. (5) yields the closed-form analytical solution

$$\alpha_F(0) = \frac{\alpha'_F(0)}{\Gamma_c} = [1 + \Gamma_c I_z(\infty)]^{-1}\alpha_s = \frac{\alpha_s}{1 + \tilde{\Gamma}_c} \tag{13}$$

where

$$I_z(\infty) \equiv \int_0^\infty \exp\left(-Sc \int_0^\infty f \, dn\right) \cong \left(0.47 S^{\frac{1}{3}} c\right)^{-1} \tag{14}$$

and $\tilde{\Gamma}_c = \Gamma_c/f''(0)Sc^{1/3} \cong \Gamma_c/0.47Sc^{1/3}$. The companion expression for the wall temperature gradient, from Eq. (6), is found to be

$$\theta'_F(0) = Pr^{\frac{1}{3}} f''(0) \cong 0.47 Pr^{\frac{1}{3}} \tag{15}$$

which together with Eq. (13) yields from Eq. (10) the nondimensional heat transfer function

$$Q_{w,F} \approx 0.47 Pr^{\frac{1}{3}} \left[1 - \theta_w + Le^{0.67} \frac{\alpha_s h_D}{\hat{C}_p T_s} \left(\frac{\tilde{\Gamma}_c}{1 + \tilde{\Gamma}_c}\right)\right] \tag{16}$$

This expression clearly indicates that low to moderate catalysis rates can significantly reduce heat transfer when the boundary layer is well out of gas-phase equilibrium. Used in conjunction with the sweepback-dependent inviscid properties of Fig. 4, these relations serve to extend Goulard's well-known study[2] of this limit to include the influence of arbitrary sweep.

Figure 7 shows the predicted sweepback effect on the wall atom concentration α_w for several values of Γ_{C_0} ranging from completely noncatalytic ($\Gamma_{C_0} = 0$) to fully catalytic ($\Gamma_{C_0} \gg 1$). It is seen that the influence of sweep in reducing the Dähmkohler number is rather small, causing only a slight increase in α_w when Γ_{C_0} is of order unity. Far more significant is the influence of the reduction in α_s with sweep, which correspondingly reduces α_w such that it vanishes for sweep angles above 60 deg. The same trend is also reflected in the corresponding sweepback effect on heat transfer, as shown in Fig. 8

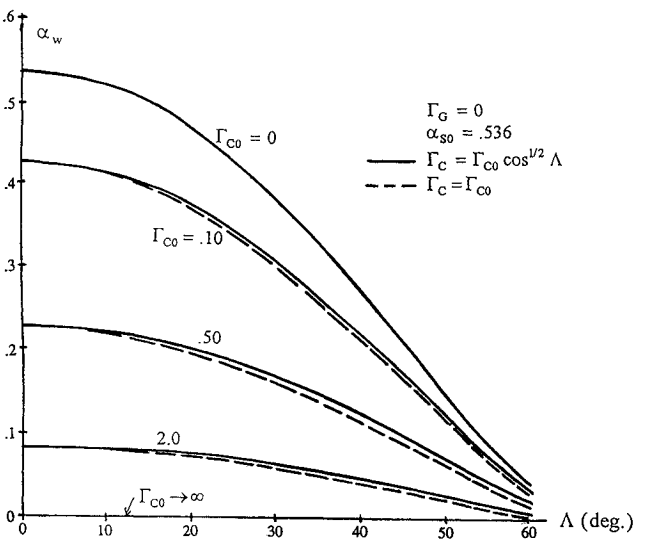

Fig. 7 Sweepback effect on wall atom concentration for frozen gas-phase flow.

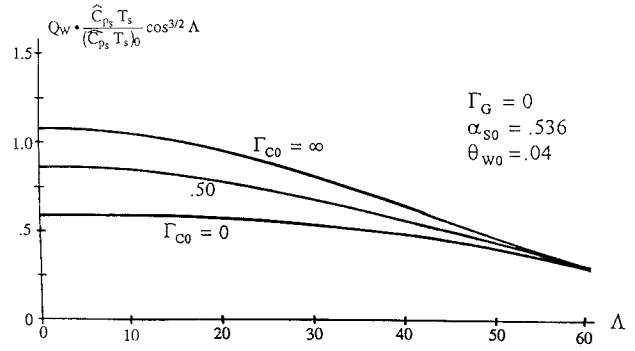

Fig. 8 Sweepback effect on heat transfer in frozen flow.

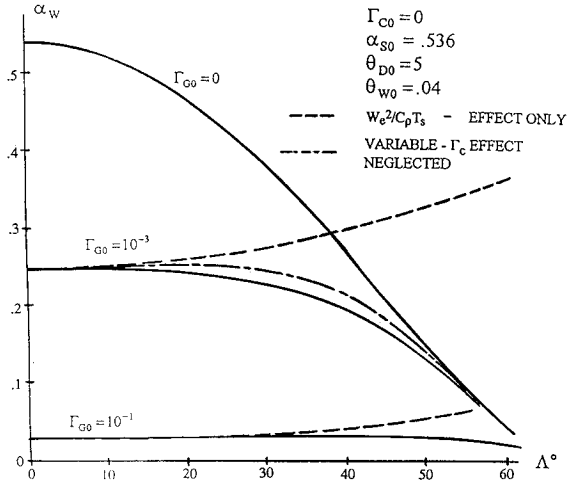

Fig. 9 Sweepback effect on nonequilibrium atom concentration at a noncatalytic wall.

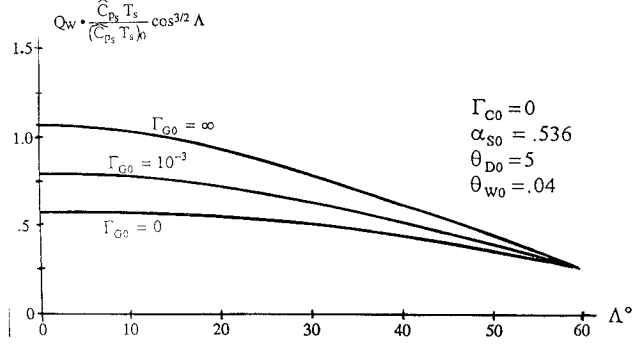

Fig. 10 Sweepback effect on nonequilibrium heat transfer to a noncatalytic wall.

[note here that we have plotted $\dot{q}_w$, which reflects the additional sweep effects on $\hat{C}_p T_s$ and $\rho_w \mu_w \beta_s \sim \cos^{3/2}$ multiplied through from the denominator of Eq. (10)]. The overall aerothermochemical effect of sweep is clearly seen: it wipes out the dissociation effects altogether beyond $\Lambda = 60$ deg, such that the considerable beneficial effect of a noncatalytic wall in reducing zero sweep heat transfer is completely eliminated, leaving only the usual ideal gas sweep-reduction effect proportional to $\sim(\hat{C}_p T_s/\hat{C}_{p_0} T_{s_0}) \cos^{3/2} \Lambda$.

Nonequilibrium Boundary-Layer Flow

Turning to the effects of finite-rate chemistry ($\Gamma_G \neq 0$), purely numerical solutions are necessary as described earliar. Results for α_w vs Λ on a noncatalytic wall for various values Γ_{G_0} are plotted in Fig. 9 so as to show the individual contributions of the various factors already described. Solutions for cases with small to moderate nonzero values of Γ_c were also obtained but are not presented here because of space limitations. It is seen that notwithstanding the significant spanwise viscous dissipation heating effect on the reaction rates (especially dissociation), which alone tends to increase α_w significantly with sweep, the counterbalancing effects from the reduction in α_s and T_s (especially the attendant rise in $\theta_D \sim T_s^{-1}$) are even stronger with the net result that sweep diminishes the gas-phase dissociation effect to virtually zero beyond $\Lambda = 60$ deg. Qualitatively, the role of sweep is, thus, the same as found for catalytic surface reaction. The corresponding nonequilibrium heat transfer variations with sweep are presented in Fig. 10 and mirror the same conclusions.

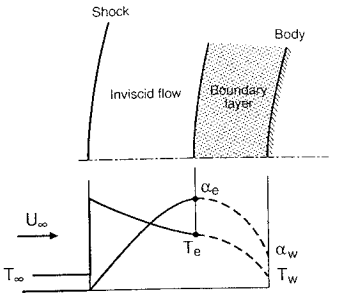

Fig. 11 Nonequilibrium shock layer flow at lower Reynolds numbers, schematic.

Concluding Remarks

The present study provides physical insight as to how and why sweepback fundamentally alters the nonequilibrium dissociation effects on stagnation line heat transfer when finite catalytic atom recombination is present on the body surface. The results also provide a heretofore unavailable computational database for the checkout of any future studies of swept nonequilibrium flows. Furthermore, our findings have an important bearing on the design of thermal protection systems for hypersonic vehicles. In particular, the prediction that large sweep eliminates the favorable heating reduction effect of a noncatalytic surface would suggest that efforts to lower surface catalycity (however effective elsewhere on the vehicle) would have little impact on the highly swept wing leading-edge region.

The present work offers a basis for future interesting parametric studies, such as the influence of wall temperature ratio and the characteristic dissociation temperature parameter θ_D on the foregoing conclusions regarding the effects of sweep. Another very desirable extension would be the inclusion of further nonequilibrium effects in the inviscid flow as encountered at very high-altitude (low-Reynolds number) flight conditions above roughly 250,000 ft altitude where the boundary layer has thickened to occupy a significant portion of the shock layer (Fig. 11).

Appendix: Inviscid Dissociated Flow Properties with Sweep

We suppose that the inviscid equilibrium values of stagnation pressure, temperature, and degree of dissociation for zero sweep (p_{s_0}, T_{s_0}, and α_{s_0} respectively) are known for each desired altitude and flight speed as obtained from a standard normal shock table.[10] Then the relative effects of sweep on these values can be determined as follows for hypersonic speeds where the freestream ambient energy $\hat{C}_{p_\infty} T_\infty \ll U_\infty^2/2$.

The steady flow energy equation requires that

$$\hat{C}_{p_s} T_s = \frac{1}{2} U_\infty^2 \cos^2 \Lambda \Big/ \left(1 + \frac{\alpha_{s_0} R_M}{\hat{C}_{p_0}} \theta_{D_0}\right)$$

which in turn implies the ratio

$$\frac{\hat{C}_{p_s} T_s}{\hat{C}_{p_0} T_{s_0}} = \left(1 + \frac{\alpha_{s_0} R_M}{\hat{C}_{p_0}} \theta_{D_0}\right) \cos^2 \Lambda - \frac{\alpha_s R_M}{\hat{C}_{p_0}} \theta_{D_0} \qquad \text{(A1)}$$

Using the value of the dissociated gas mixture specific heat that $\hat{C}_p/R_M \cong 7(1-\alpha_s)/2 + 5\alpha_s$ (which is weighted toward cold-wall zero vibration conditions), we further have that

$$\frac{\hat{C}_{p_s}}{\hat{C}_{p_0}} \cong \frac{7 + 3\alpha_s}{7 + 3\alpha_{s_0}} \qquad \text{(A2)}$$

Finally, from the equilibrium dissociation relationship (law of mass

action) in which we take $C_D = p_{s_0}\alpha_{s_0}^2 e^{\theta_{D_0}}/(1-\alpha_{s_0}^2)$ there is obtained the equation governing α_s that

$$\frac{\alpha^2}{1-\alpha_s^2} = \left(\frac{\alpha_{s_0}^2}{1-\alpha_{s_0}^2}\right)\sec^2\Lambda e^{\theta_{D_0}-\theta_D} \tag{A3}$$

where we have used $p_s/p_{s_0} \cong \cos^2\Lambda$ and where it is noted that $\theta_D = T_{s_0}\theta_{D_0}/T_s$. A simultaneous solution of Eqs. (A1–A3) for $\Lambda > 0$ then yields the sweep effect on $\hat{C}_p$, T_s, α_s, and then θ_D for a given set of the unswept parameters.

With the foregoing in hand, the crossflow viscous dissipation heating parameter can then be determined using $w_e^2 = U_\infty^2 \sin^2\Lambda$ as

$$\frac{w_e^2}{2\hat{C}_p T_s} = \frac{U_\infty^2 \sin^2\Lambda}{2\hat{C}_p T_s} = \left(1 + \frac{\alpha_s h_D}{C_p T_s}\right)\tan^2\Lambda \tag{A4}$$

with $h_D/\hat{C}_p T_s = 2\theta_D/(7+3\alpha_s)$.

References

[1]Fay, J. A., and Riddell, F. R., "Theory of Stagnation Point Heat Transfer in Dissociated Air," *Journal of the Aeronautical Sciences*, Vol. 25, No. 2, 1958, pp. 73–85.

[2]Goulard, R. J., "On Catalytic Recombination Rates in Hypersonic Stagnation Heat Transfer," *Jet Propulsion*, Vol. 28, No. 11, 1958, pp. 737–745.

[3]Chung, P. M., "Hypersonic Viscous Shock Layer of Nonequilibrium Dissociating Gas," NASA Rept. R-109, May 1961.

[4]Inger, G. R., "Nonequilibrium Stagnation Point Boundary Layers with Arbitrary Surface Catalyticity," *AIAA Journal*, Vol. 1, No. 8, 1963, pp. 1776–1784.

[5]Lees, L., "Laminar Heat Transfer Over Blunt-Nosed Bodies at Hypersonic Flight Speeds," *Jet Propulsion*, Vol. 26, No. 4, 1956, pp. 259–268.

[6]Reshotko, E., "Heat Transfer to a General Three-Dimensional Stagnation Point," *Jet Propulsion*, Vol. 28, No. 1, 1958, pp. 58–60.

[7]Hayes, W. D., and Probstein, R. F., *Hypersonic Flow Theory*, Academic, New York, 1959, pp. 293–312.

[8]Moran, J., *An Introduction to Theoretical and Computational Aerodynamics*, Wiley, New York, 1984, pp. 289–295.

[9]Reshotko, E., and Beckwith, I. E., "Compressible Laminar Boundary Layer Over a Yawed Infinite Cylinder with Heat Transfer and Arbitrary Prandtl Number," NACA Rept. R-1379, June 1957.

[10]Wittliff, C. E., and Curtis, J. T., "Normal Shock Wave Parameters in Equilibrium Air," Cornell Aeronautical Lab., Rept. CAL-111, Buffalo, NY, June 1961.